Supporting Information

Formation characteristics of aerosol triplet state and coupling effect between the separated components with different polarity

Dongjie Guan[a], Qingcai Chen[a*], Jinwen Li[a], Hao Li[a], Lixin Zhang[a], Yuqin Wang[a], Xiaofei Li[a] and Tian Chang[a]

[a] *School of Environmental Science and Engineering, Shaanxi University of Science and Technology, Xi'an 710021, China*

*Corresponding authors:

*(Q. C.) Phone: (+86) 0029-86132765; e-mail: chenqingcai@sust.edu.cn; School of Environmental Science and Engineering, Shaanxi University of Science and Technology, Weiyang District, Xi'an, Shaanxi, 710021, China;

List of contents:

Number of pages	**25**
Text	**3**
Table	**5**
Figure	**19**

Text S1. Sample preparation and information

The actual $PM_{2.5}$ sample collection site is Shaanxi University of Science and Technology, Weiyang District, Xi'an, China. The surrounding environment of the school is mainly university parks and residential areas. There is Daming Palace building materials market in the south of the campus, and there is no major industrial emission source. **Fig.S1** shows the location information map of the sampling points. During the sampling period, there was no rain or snow and other weather, but all were affected by haze. The air quality situation on that day is shown in **Table S1**.

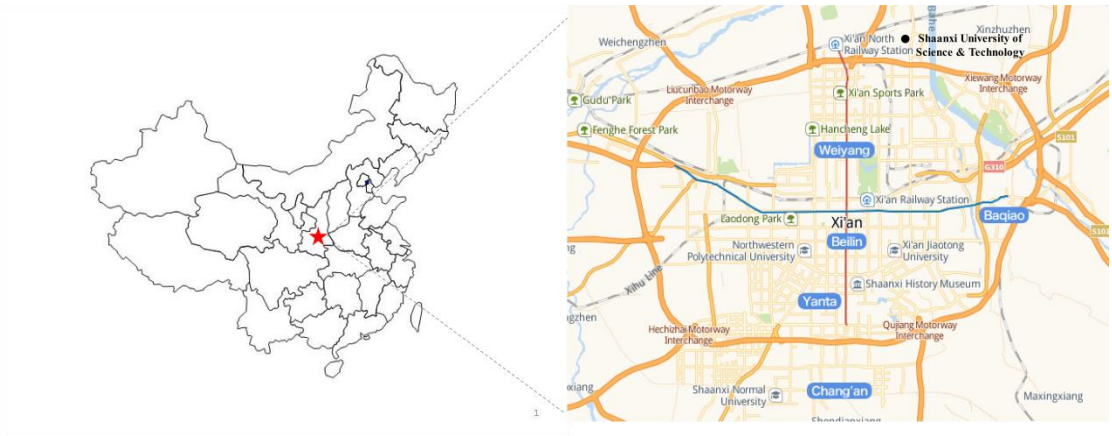

Fig.S1. Sampling point location and surrounding environment in this study. Imagery © 2021 Google, map data © 2021 Google.

Table S1. Air quality information on the day of sampling.

Date	$PM_{2.5}$	SO_2	NO_2	CO	O_3
2019/12/21	200	14	87	1.75	9
2019/12/25	157	10	47	1.63	11
2020/1/3	156	22	80	1.66	14
2020/1/9	181	11	49	2	5
2020/1/13	161	14	61	1.73	16
2020/1/16	169	11	55	1.82	9
2020/1/18	191	8	68	1.68	15
2020/1/23	223	14	58	1.9	26
2020/1/25	225	12	24	1.75	46
2020/2/1	138	17	31	1.49	63

The preparation of simulated combustion samples is based on a platform built by the laboratory (as shown in **Fig.S2**), which mainly includes tube furnace, air dilution box, sampling device, and air compressor. The primary organic aerosol (POA) used in the follow-up study was obtained by collecting the particulate matter produced by the combustion of the above five raw materials. The specific sample combustion process is as follows: the naturally dried raw materials are crushed, weighed, and then placed in a tube combustion furnace to simulate combustion. The combustion temperature of biomass raw materials is set to 500 ℃, and the combustion time is 1 h; the coal combustion temperature is set to 700 ℃, and the combustion time is 1.5 h. In order to ensure that the sample material is fully burned, dry air is introduced into the combustion furnace at a flow rate of 2 L min^{-1}, and the sampling pump starts sampling at the same time. The sampling flow rate is 15 L min^{-1} (the sampling pump is turned on for sampling at the same time as the sample is injected, so the combustion time is also the sampling duration). In order to simulate the formation of atmospheric particulate matter, after the flue gas produced by combustion enters the air collecting box, filtered and dried air is introduced into the box at a flow rate of 2 m^3 h^{-1} to dilute the flue gas produced by combustion. The diluted flue gas will go through the process of coalescence and sedimentation, part of which is collected, and the remaining part is discharged through a fume hood. The flue gas passes through the $PM_{2.5}$ cutting head to obtain fine particulate matter samples, which are finally enriched on a quartz filter membrane (Pall life sciences) with a diameter of 47 mm. The collected filter membrane is stored in a refrigerator at -20 ℃ for later use. After changing the raw materials in each experiment, clean the entire experimental device with dry clean air and purge for 30 min to remove residual particles. Each kind of combustion raw material was fired and collected twice as parallel samples. **Table S2** is the information of combustion samples.

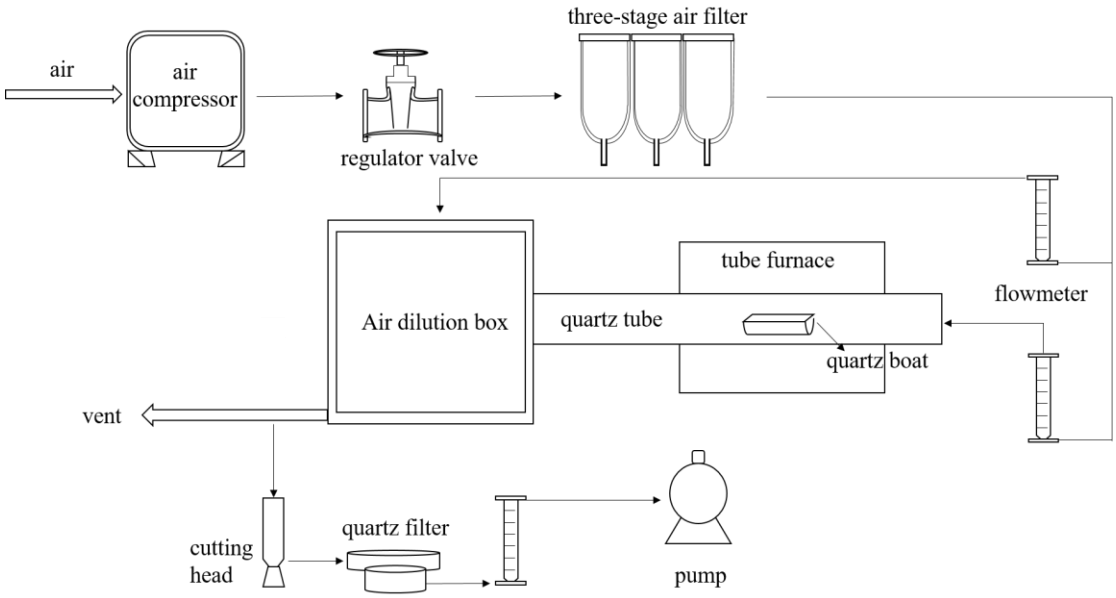

Fig.S2. Schematic diagram of combustion simulation device.

Table S2. Information table of combustion samples.

Sample	Raw material weight (g)	Burning temperature (℃)	Sampling duration (h)
Wheat-straw1	2.79	500	1
Wheat-straw2	2.81		
Rice-straw1	2.81		
Rice-straw2	2.47		
Wood1	2.85		
Wood2	2.55		
Bituminous coal 1	6.54	700	1.5
Bituminous coal 2	6.73		
Brown coal 1	12.71		
Brown coal 2	13.28		

According to previous research reports, the water-soluble extract can be further separated by the SPE column, and finally separated into the low-polarity part (HP-WSM) and the medium-polarity part (HULIS).[1,2] In this study, the SPE column with C-18 as the filler was selected (Agela, 500 mg, 6 mL). The specific separation process uses a solid phase extraction device (**Fig.S3**). First connect the extraction device and install the SPE column.

Fig.S3. SPE column and solid phase extraction device.

(1) Take a certain volume from the filtered WSM and put it in a clean brown glass bottle to wait for separation; (2) In order to activate the active groups in the SPE column, remove the adsorbed impurities that affect the analysis, and balance the SPE column to provide a good adsorption environment for the sample, the SPE column must be activated before separation. Use 1 column volume of methanol and 2 column volume of ultrapure water in sequence. It is worth noting that the activated SPE column must be kept moist before loading, otherwise the recovery rate will be low and the reproducibility will be poor; (3) Pour the WSM solution sample prepared in advance into the SPE column, connect the lower end of the column with a glass bottle, which will drop naturally under the action of gravity, and the sample directly flowing out of the column is a highly polar water-soluble substance (HP-WSM). The adsorbed substance in the packing is HULIS. After the separation of all the solutions is completed, use a vacuum pump for 3 minutes to drain the water in the column. Then add 10 mL of methanol (into twice) to completely immerse the methanol in the packing, and flicking the wall of the tube can better extract HULIS. After soaking for 5 minutes, open the valve and let the sample flow into a clean glass bottle. Finally, vacuumize for 3 minutes. At this stage, the HULIS dissolved in methanol is obtained; (4) The methanol-dissolved HULIS sample was concentrated using a rotary evaporator, the volume was concentrated to about 1 mL. Transferred to a brown vial, and then the beak bottle used by the evaporator was cleaned with a little methanol three times. This process is to minimize the loss of HULIS, to prevent it from hanging on the wall. Finally control the volume of the solution in the brown vial within 2 mL, then dry it with nitrogen. At the last, add 3 mL of ultrapure water to re-dissolve to obtain HULIS dissolved in water. The sample solution is stored at 4 ℃ until use. The information of the prepared sample solution is shown in **Table S3**.

Table S3. Preparation information table of different polar components of samples.

Sample type	Sample number	WSM (Number of membranes/membrane diameter/volume of solvent) (piece/mm/mL)	MSM (Solvent amount) (mL)	HULIS Volume after separation (mL)	HP-WSM Volume after separation (mL)
Atmospheric PM2.5 samples in winter	2019/12/21	30/10/21	21	3.3	21
	2019/12/25	52/10/21	21	3	21
	2020/1/3	25/10/21	21	3	21
	2020/1/9	52/10/21	21	3	21
	2020/1/13	52/10/21	21	3	21
	2020/1/16	48/10/21	21	3	21
	2020/1/18	36/10/25	25	3	25
	2020/1/23	24/10/21	21	3	21
	2020/1/25	40/10/21	21	3	21
	2020/2/1	38/10/21	21	3	21
combustion simulation sample	Wheat-straw1	18/6/10	10	3	10
	Wheat-straw2	18/6/10	10	3.1	10
	Rice-straw1	18/6/10	10	3	10
	Rice-straw2	18/6/10	10	3	10
	Wood1	18/6/10	10	3	10
	Wood2	18/6/10	10	3	10
	coal 1	60/6/25	10	1	10
	coal 2	60/6/25	10	1	10

Text S2. Photochemical experiment

The photochemical experiment is carried out using a photo-simulation reactor, as shown in **Fig.S4**, which is a reactor built and assembled by the research group used in this research. The reactor is used to provide a good photochemical reaction environment. The reactor is customized from high-purity quartz, equipped with the same high-purity quartz cover, and matched with rubber gaskets to achieve a sealing effect. At the same time, there are two interfaces in the upper and lower parts of the reactor, and the upper part is a vent, which provides a corresponding gas environment for experiments that require a pure gas environment. The lower part is the water port, the water port is connected to the cold water circulation machine, and the temperature of the circulation machine is set to 7 ℃. At this time, the temperature and humidity in the reactor are about 25 ℃ and 50% respectively, which simulates the normal actual atmospheric environmental conditions. Below the reactor is a magnetic stirrer, which is used to mix the cooling water in the reactor in time to make the temperature and humidity in the reactor evenly distributed, and the speed is set to 200 rmp/min; there is a sample stage in the reactor, which can be used for sample reaction dishes.

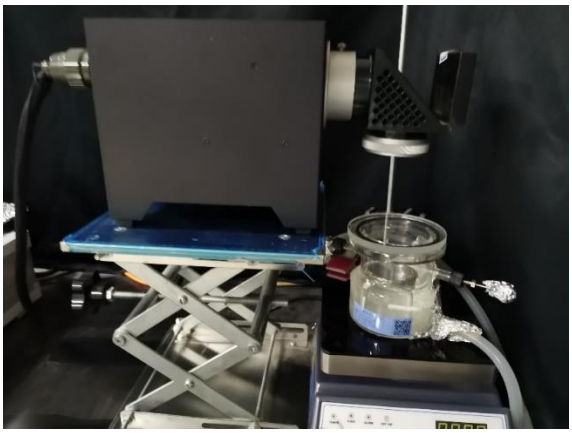

Fig.S4. Photochemical simulation reaction device**.**

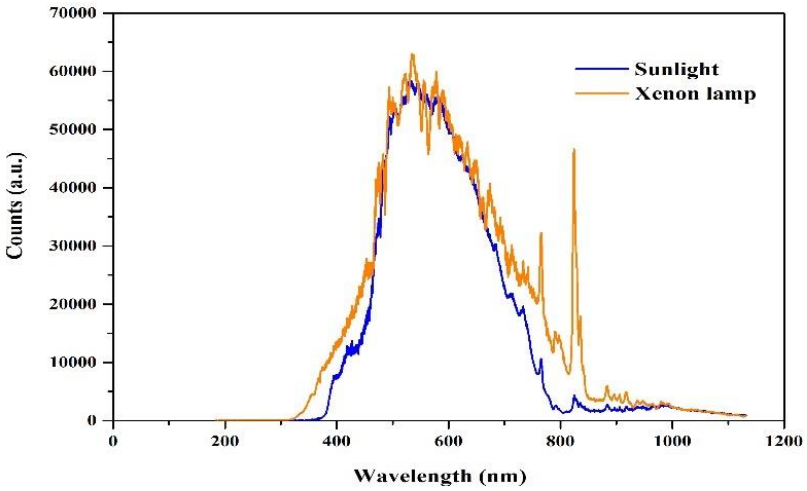

Fig.S5. Spectral characteristics of xenon light source.

During the experiment, all samples were placed in a special quartz reaction dish, as shown in **Fig.S6**. The inside of the reaction vessel is cylindrical with a diameter of 12 mm and a thickness of 2 mm. The openings on both sides have a diameter of 1 mm and are equipped with PTFE sealing plugs to ensure a sealed environment. The overall triplet experiment is divided into three parts, including TMP quenching $^{3}C^{*}$ process, FFA quenching $^{1}O_{2}$ and $^{1}O_{2}$ quenching process after adding SA. Involving 88 samples of different polarities (40 actual samples, 40 biomass burning samples, and 8 coal burning samples), 1 group of parallel, and 3 groups of blank backs. The concentration of the sample solution used in this part of the experiment was adjusted to 20 mg-C/L, and the original concentration of TMP and FFA were both 40 μM/L. In the experiment, first mix the sample solution and quencher (TMP, FFA) in equal volumes (add 10 μL of SA quencher when performing FFA experiment, and the SA concentration after mixing is 1mM). Set a series of (0, 5, 10, 15, 30, 50, 90), and take 120 μL sample for illumination. After the corresponding time of illumination, take a sample (90 μL) and analyze it by HPLC. Up to 6 reaction dishes can be placed on the sample stage, independent of each other and not affected, and the light is evenly received.

Fig.S6. Triplet photochemical reaction dish.

Using the relationship between the specific peak area and the concentration of the target substance, a standard curve of the concentration of the test substance (as shown in **Fig.S7**) is used to correct the measurement deviation. In addition, this study also proved that the pure quencher solution is hardly photolyzed under light (as shown in **Fig.S8**), which is the same as the previous research report3. In this study, the relative standard deviation of the TMP concentration of the parallel samples was 2.5%, and the relative standard deviation of the FFA concentration was 3.3%.

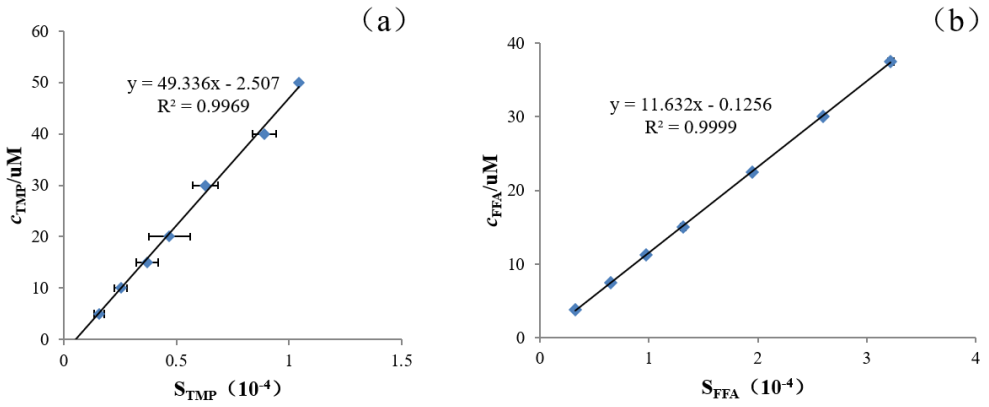

Fig.S7. (a) Standard curve of TMP concentration; (b) Standard curve of FFA concentration.

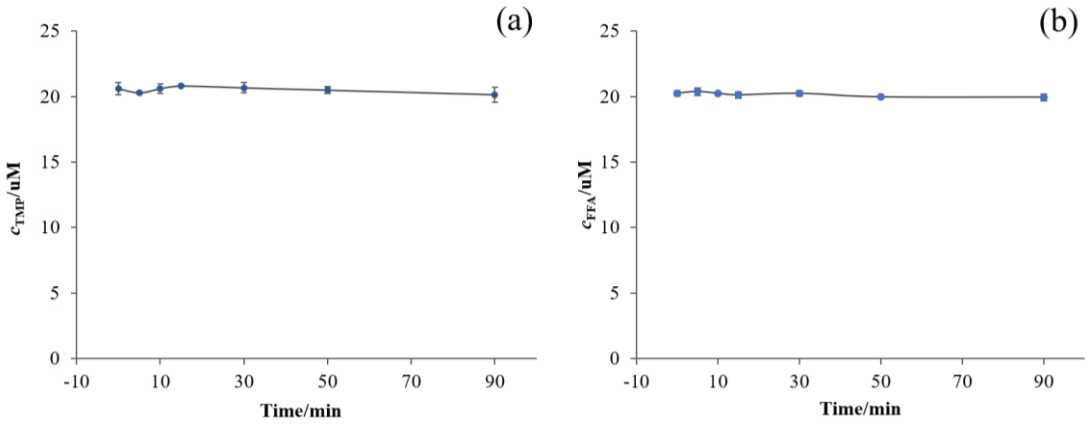

Fig.S8. (a) Photolysis of TMP solution; (b) Photolysis of FFA solution.

Text S3. ^{3}C*quantum yield coefficient calculation

Studies have shown that the process of quenching the triplet state conforms to the pseudo-first order reaction kinetics, and the fitting method is shown in the following formula. In order to calculate the triplet quantum yield coefficient yield (f_{TMP}) and the quantum yield of singlet oxygen (Φ_{1O2}) in the atmospheric environment, it is necessary to fit the k_{TMP} (the relationship between the concentration of TMP and the light time using the first-order kinetic equation:

$$c_{\mathrm{TMP}}/a = \exp(-k_{TMP}t) \quad (1)$$

k_{TMP}——TMP decay rate constant (min^{-1});

c_{TMP}——TMP concentration (μmol L^{-1});

t——Light time (min).

Similarly, the quenching process of the singlet oxygen quenchers FFA and $^1O_2$ also conforms to the pseudo-first order reaction kinetics, and the same equation is used to fit.

Quantum yield refers to the utilization efficiency of photons in a photochemical reaction. The quantum yield of a photochemical reaction can be defined as the number of molecules of the reactant produced by absorbing a quantum. That is, the quantum yield = the number of molecules of the product/absorbed Quantum number. In an actual reaction, the quantum yield (Φ_i) of the reactant is equal to the rate of formation of the product (R_i, mol/L/s) divided by the rate of light absorption (R_a, einsteins/cm3/s). The calculation formula is as follows [4, 5]:

$$\Phi_i = R_i/R_a \quad (2)$$

$$R_a = \sum_\lambda \frac{I_\lambda(1-10^{-A_\lambda})}{l} \quad (3)$$

I_λ ——the photon flux at λ wavelength (einsteins cm^{-2} s^{-1});

A_λ——the absorbance of the solution at λ wavelength;

l ——the optical path length (1 cm).

This research refers to the improved method of Laszakovits et al.[6] Use 4-nitroanisole and pyridine (PNA-pyr) standard solution system to measure photon flux, as shown in formula (4) , (5):

$$I_\lambda = \frac{k'[PNA]_0 l}{1000\Phi(1-10^{-\varepsilon_\lambda l[PNA]_0})} \quad (4)$$

$$\Phi = 0.29[pyr] + 0.00029 \quad (5)$$

In the formula, k' is the first order reaction rate constant of the substrate attenuation of the PNA-pyr system calculated by the HPLC peak area (s^{-1}); $[PNA]_0$ is the initial molar concentration of PNA; ε_λ is the molar absorption coefficient of PNA at λ wavelength(M^{-1} cm^{-1}); l is the optical path length (1 cm); Φ is the quantum yield of ^{3}PNA* (mol $Einstein^{-1}$). In this study, the photon flux was calculated using 10 μM PNA and 10 mM pyr (concentration in the mixed reaction body). Figure S9 shows the absorbance of PNA-pyr and the kinetic fitting of the triplet quenching process.

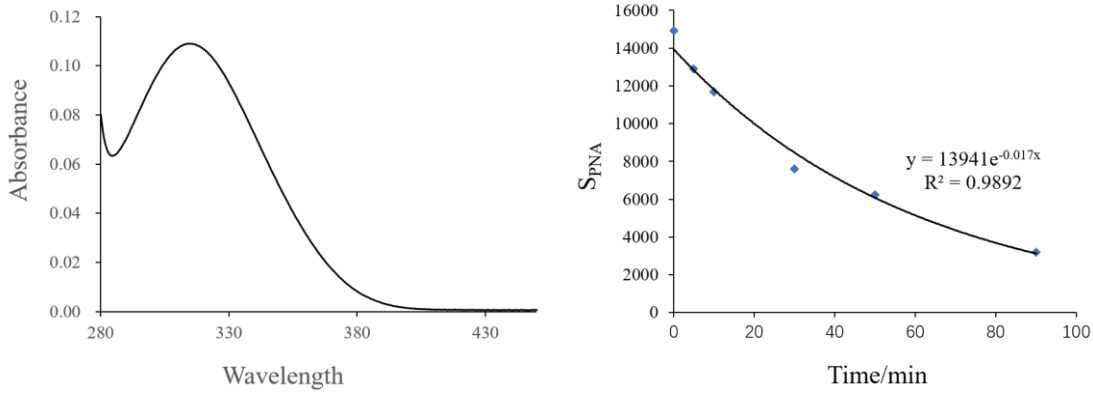

Figure S9 (a) Absorbance of PNA-pyr system; (b) Triplet dynamics fitting of PNA-pyr system.

^{3}C*quantum yield coefficient can be expressed by the following formula:

$$f_{TMP} = \frac{k'_{TMP}}{R_a} \quad (6)$$

In addition, the generation rate of singlet oxygen R_{1O2} (M/s) can be calculated using the following formula 7, 8:

$$R_{1O2} = \frac{k_{obs,FFA} \times k_d}{k_{FFA}} \quad (7)$$

In the above formula, $k_{obs,FFA}$ (s^{-1}) is the pseudo-first order reaction rate constant attenuated by FFA in photochemical experiments. k_{FFA} is the rate constant of $^1O_2$ and FFA reaction(1.2×10^8 M^{-1} s^{-1}), k_d is the rate constant of water quenching $^1O_2$ (2.4×10^5 s^{-1}). The wavelength range of optical radiation in the relevant calculations of this study is 320 nm-600 nm.

Table S4. Sample concentration of absorbance and fluorescence experiment.

Sample number	HP-WSM (mg-C L^{-1})		HULIS (mg-C L^{-1})		MSM (mg-C L^{-1})	
	Abs	Flu	Abs	Flu	Abs	Flu
2019/12/21	19.95	Same as Abs	19,94	10 times diluted than Abs	19.97	20 times diluted than Abs
2019/12/25	19.76		19.98		19.98	
2020/1/3	19.98		19.98		20.02	
2020/1/9	19,94		19.97		20.07	
2020/1/13	20.01		19.98		19.95	
2020/1/16	20.18		19.93		19.93	
2020/1/18	20.05		20.03		20.00	
2020/1/23	20.16		19.93		20.05	
2020/1/25	19.79		20.06		20.04	
2020/2/1	19.82		20.08		19.86	
Wheat-straw1	19.85		19.72		20.01	
Wheat-straw2	20.19		19.79		20.08	
Rice-straw1	20.17		19.72		20.33	
Rice-straw2	20.13		20.03		20.20	
Wood1	19.95		19.98		20.21	
Wood2	19.82		20.08		20.08	
Coal 1	19.94	10 times diluted than Abs	20.06	100 times diluted than Abs	20.42	200 times diluted than Abs
Coal 2	19.91		19.88		19.89	

In the photochemical experiment, the initial concentration of the sample used is 20 ± 0.3 mg-C L^{-1}; Abs represents the concentration of the sample when measuring absorbance, and Flu represents the concentration of the sample when measuring fluorescence.

Table S5. k_{TMP} and Φ_{1O2} of each sample.

Sample number	HP-WSM		HULIS		MSM	
	k_{TMP} (min^{-1})	Φ_{1O2} (%)	k_{TMP}	Φ_{1O2}	k_{TMP}	Φ_{1O2}
2019/12/21	0.005	6.63	0.02	4.57	0.007	7.43
2019/12/25	0.006	5.78	0.025	7.60	0.014	11.91
2020/1/3	0.005	2.78	0.013	3.43	0.018	5.40
2020/1/9	0.006	9.23	0.021	6.45	0.033	14.37
2020/1/13	0.001	5.15	0.037	4.68	0.032	7.08
2020/1/16	0.002	6.53	0.025	6.82	0.022	8.44
2020/1/18	0.006	4.39	0.013	4.60	0.007	6.76
2020/1/23	0.008	11.92	0.01	3.57	0.015	7.03
2020/1/25	0.002	3.59	0.018	5.88	0.011	6.42
2020/2/1	0.002	6.79	0.009	5.37	0.028	8.29
Wheat-straw1	0.000	3.31	0.000	1.70	0.000	4.89
Wheat-straw2	0.000	2.18	0.000	1.49	0.000	6.34
Rice-straw1	0.000	5.97	0.001	3.09	0.005	7.10
Rice-straw2	0.000	3.66	0.001	4.66	0.004	4.75
Wood1	0.001	2.45	0.000	1.95	0.001	8.80
Wood2	0.001	2.40	0.000	3.02	0.003	7.61
coal 1	0.000	1.49	0.047	38.85	0.050	25.92
coal 2	0.000	1.47	0.054	34.18	0.062	48.77

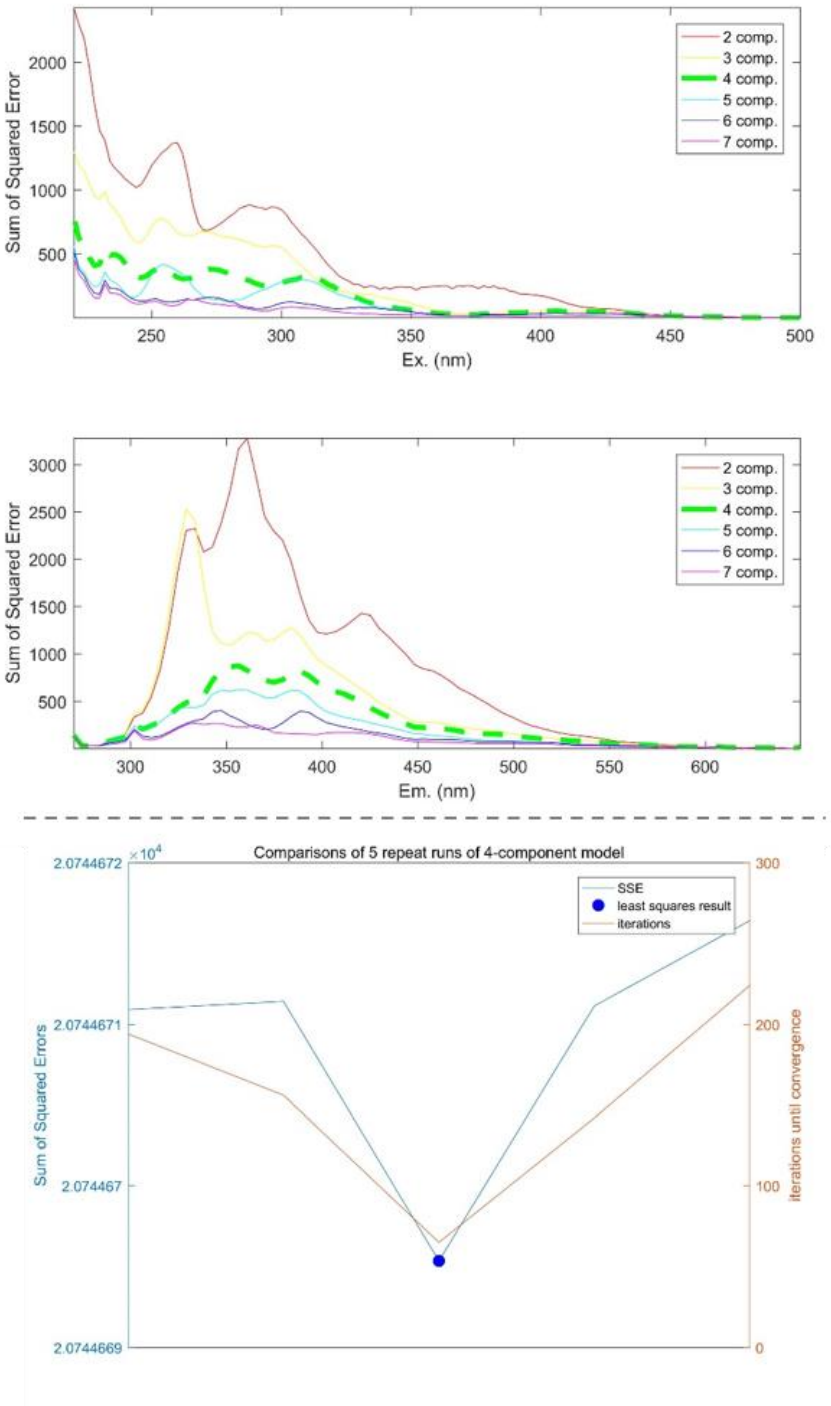

Fig.S10. PARAFAC model analysis of EEM 4 component error characteristics change trend graph.

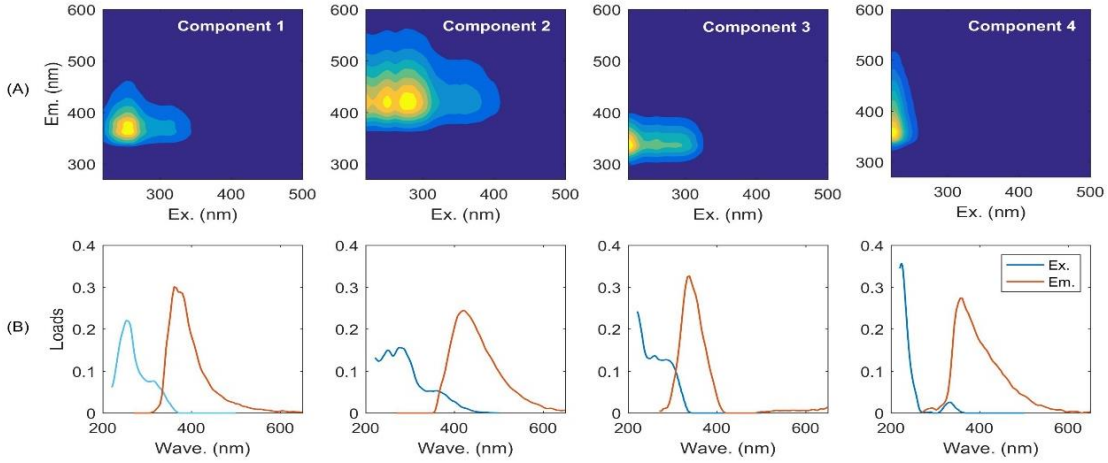

Fig.S11. (A) Four color diagrams analyzed by the parallel factor method; (b) Excitation and emission wavelengths of each chromophore.

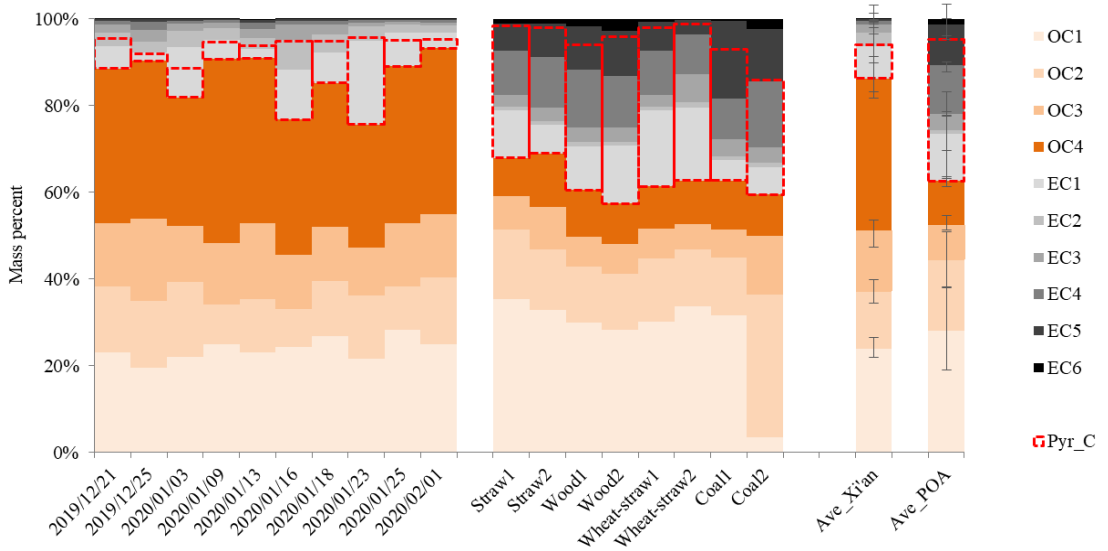

Figure S12. The composition of the carbon component of each sample.

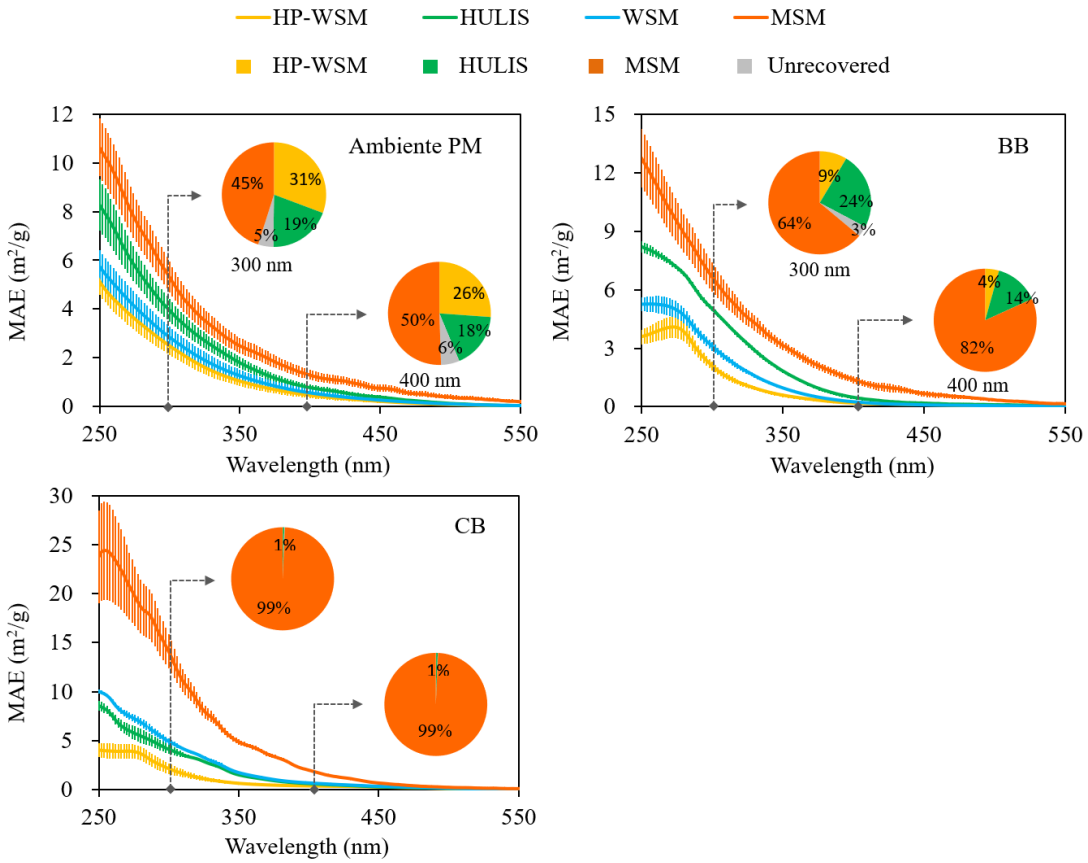

Fig.S13. The relationship between MAE and wavelength of different polar components in actual aerosols, biomass combustion, coal burning samples, and the relative contribution of different polar components at 300 nm and 400 nm.

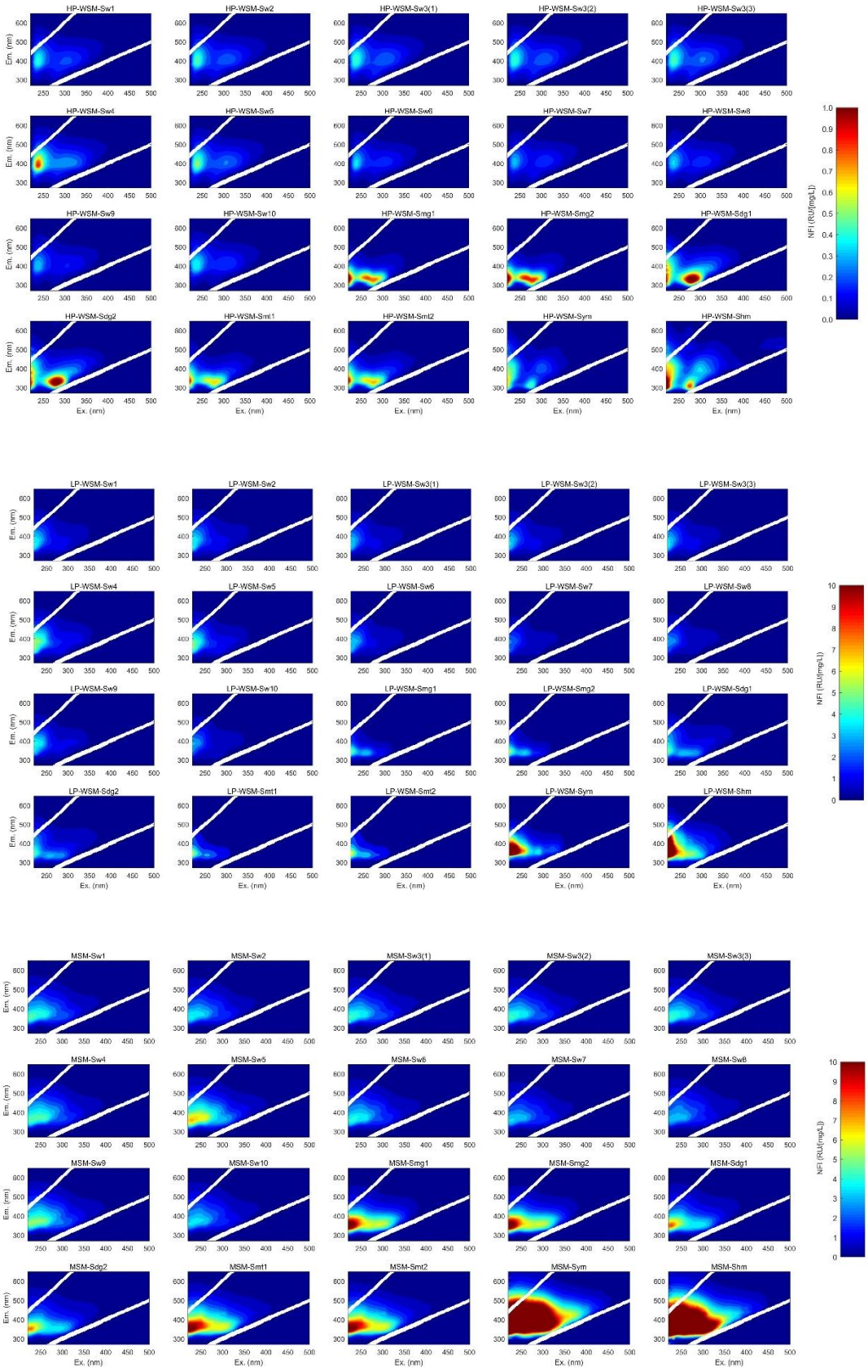

Fig.S14. Sample EEM spectrum.

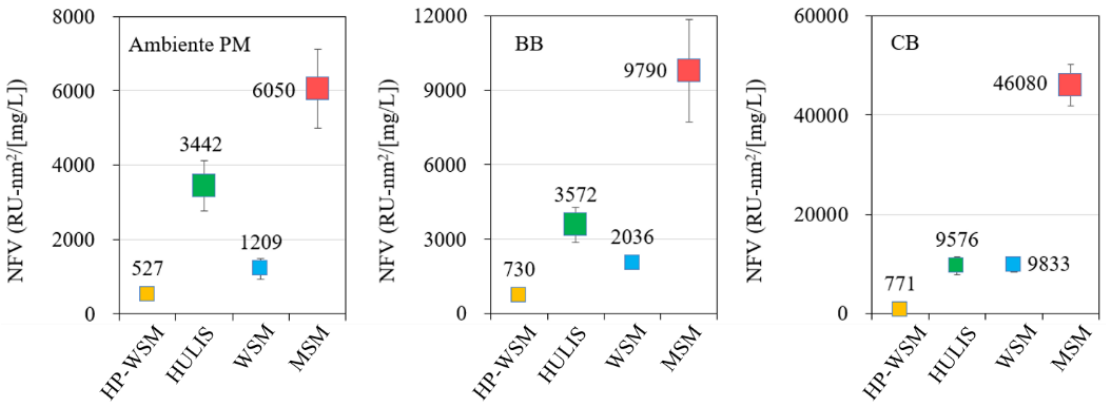

Fig.S15. NFV diagram of the different polar components of the sample.

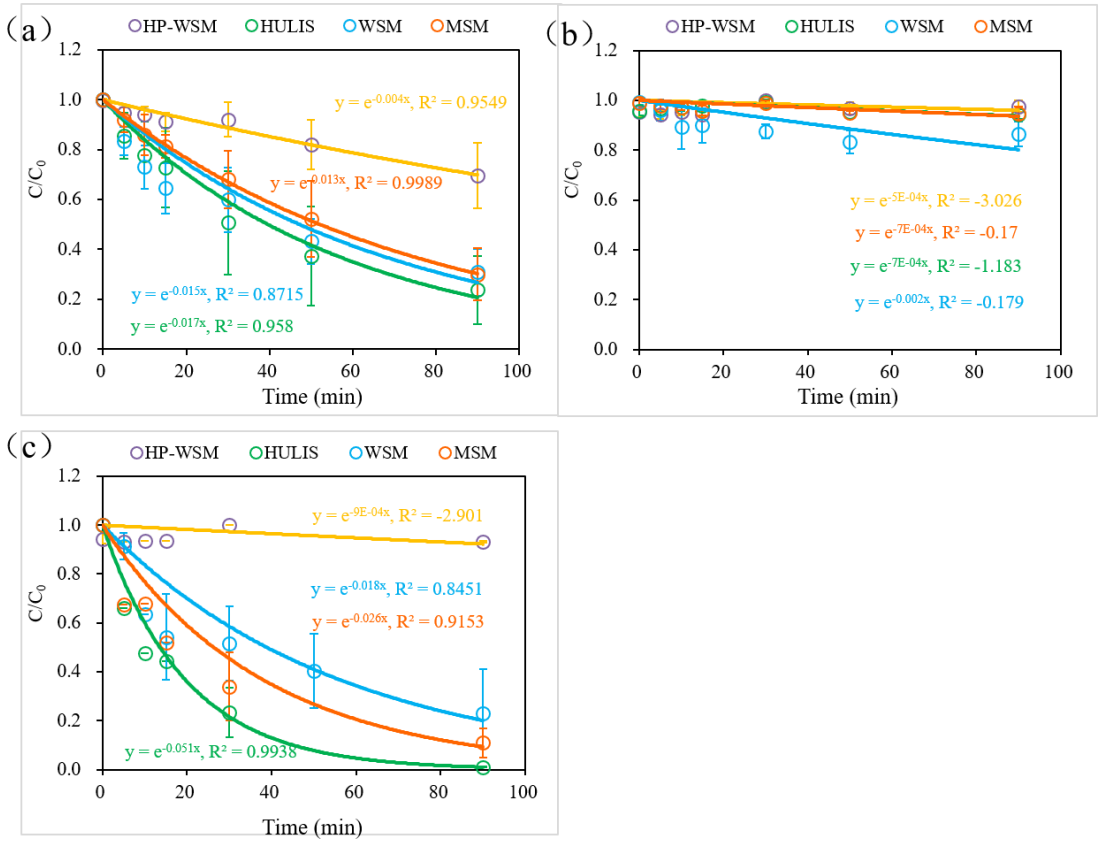

Fig.S16. Average TMP attenuation curves of different polar components, (a), (b), (c) are actual samples, biomass burning samples and coal burning samples, respectively.

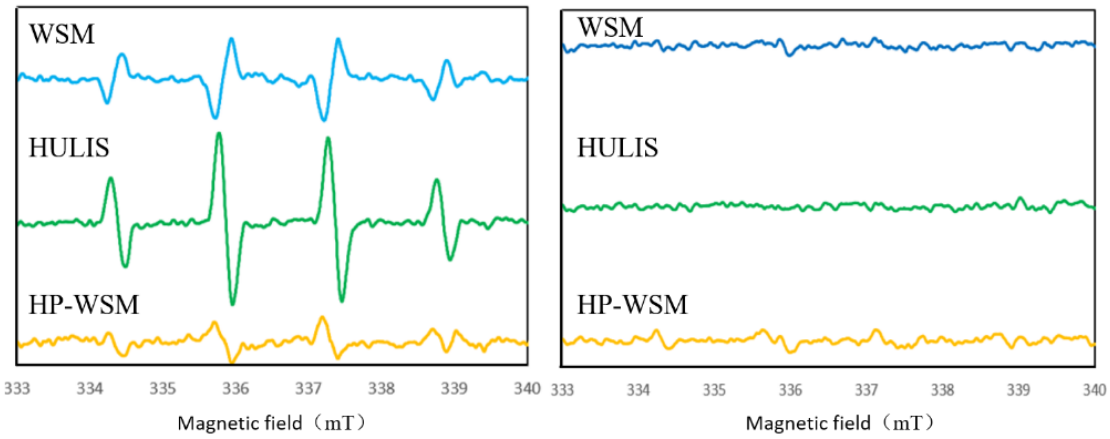

Fig.S17. ·OH signals of different polar components and their change characteristics after quenching $^1O_2$.

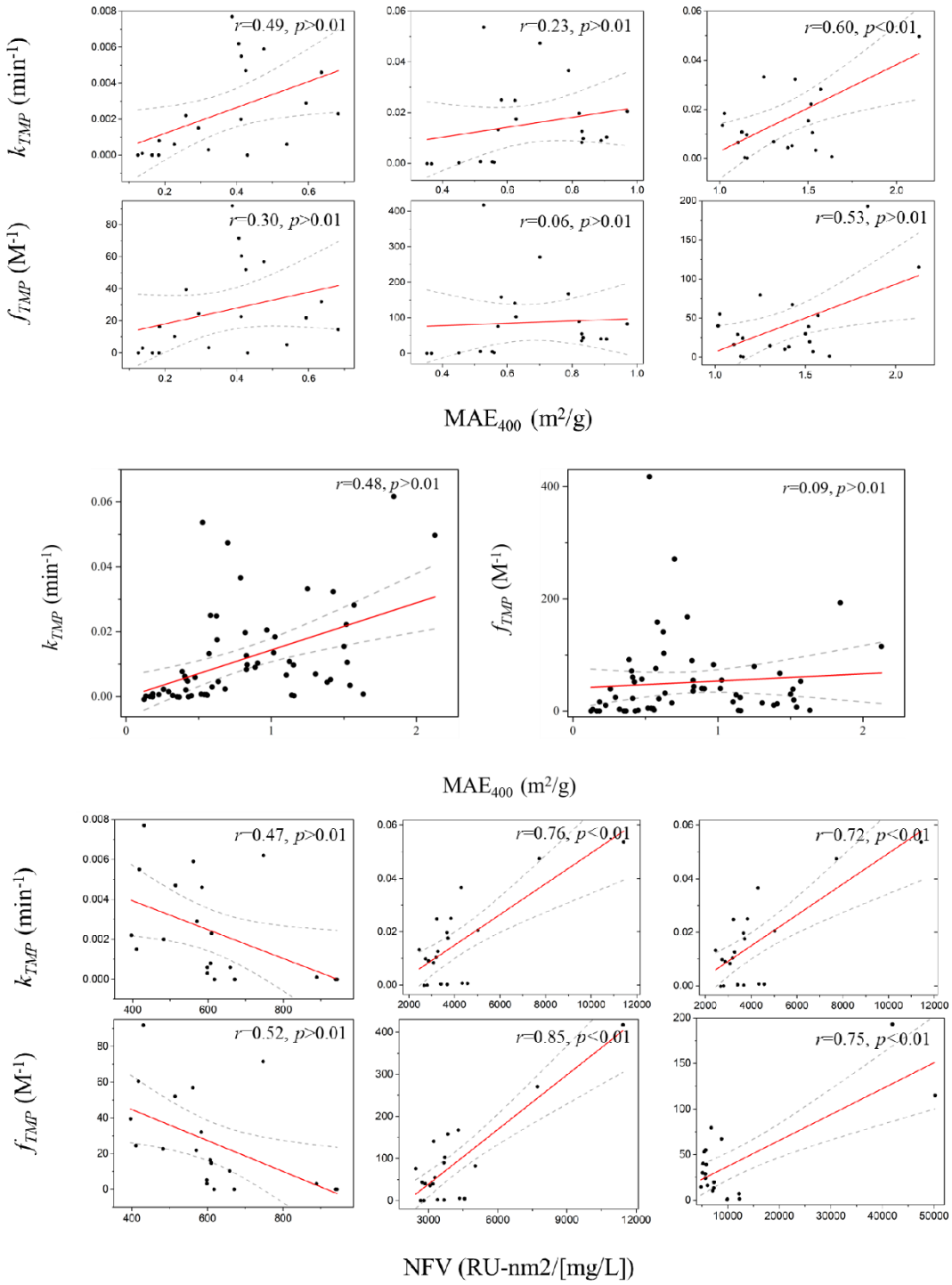

Fig.S18. Correlation between k_{TMP}, f_{TMP} and MAE_{400}, NFV, C1-C4 chromophores (Note: The left, middle and right are HP-WSM, HULIS, MSM components respectively).

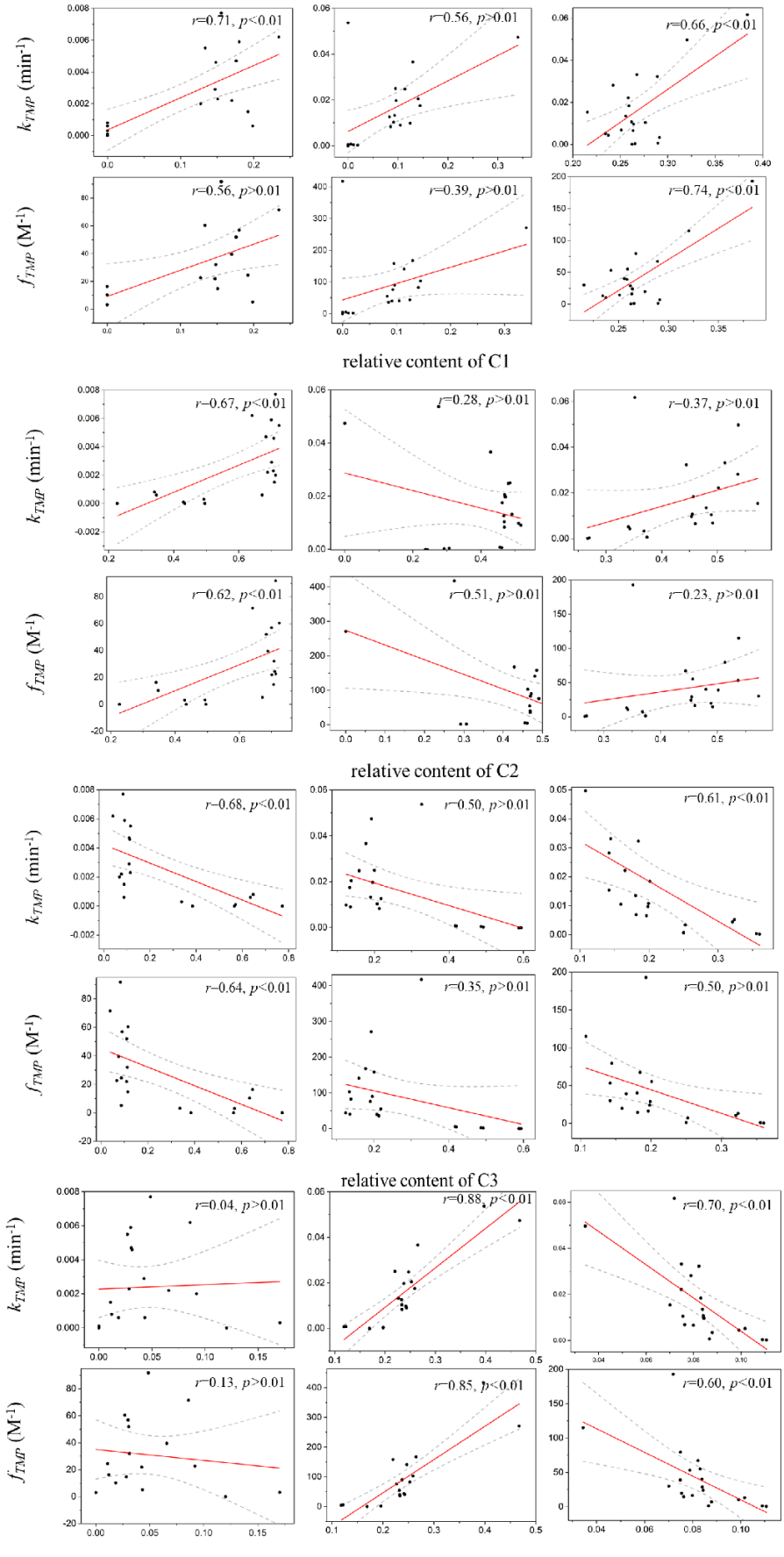

Fig.S18. (Continuous).

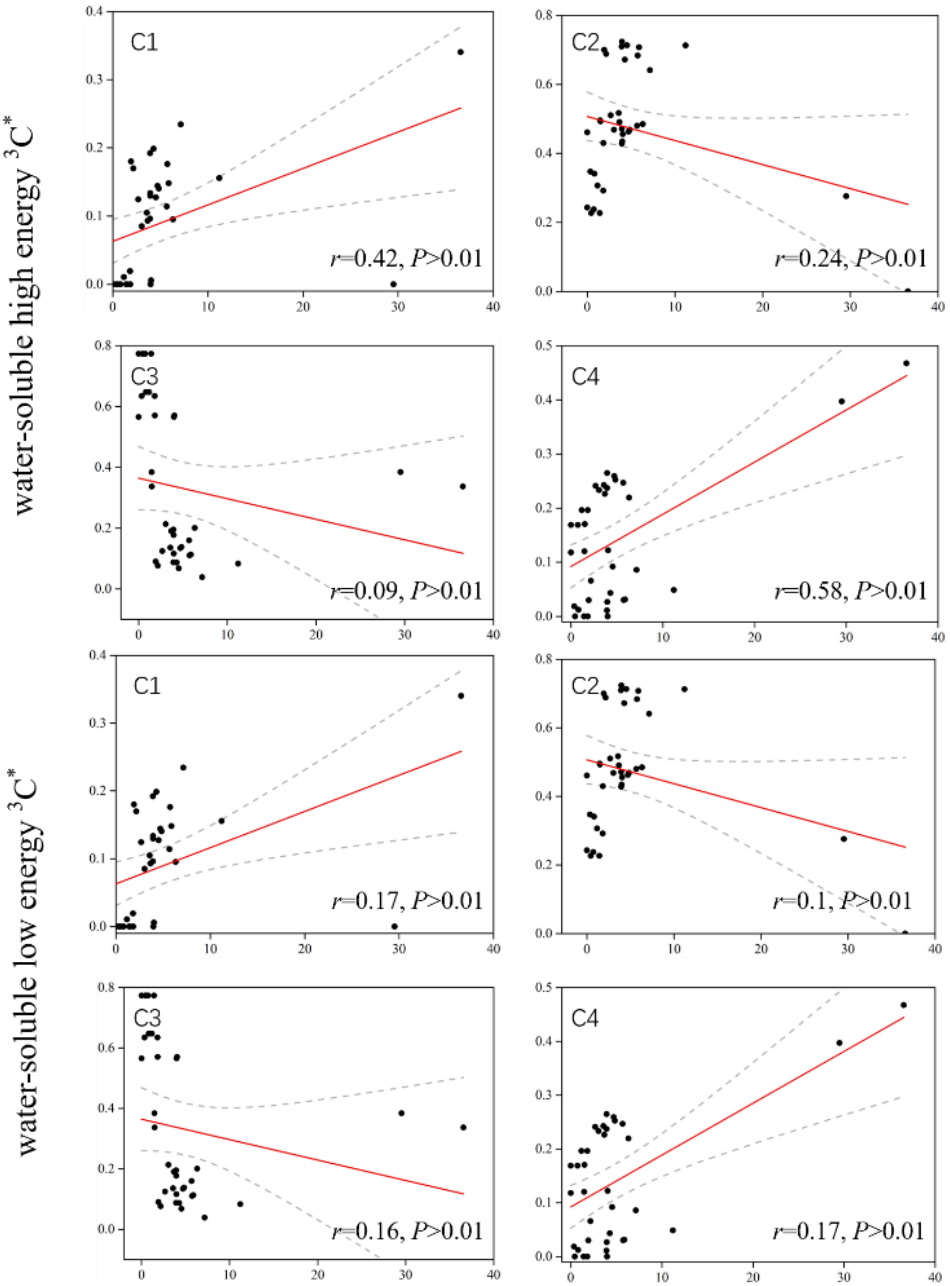

Fig.S19. Correlation between $^3C^*$ energy and C1-C4 chromophore content (Note: The horizontal axis of each figure represents the relative content of chromophores).

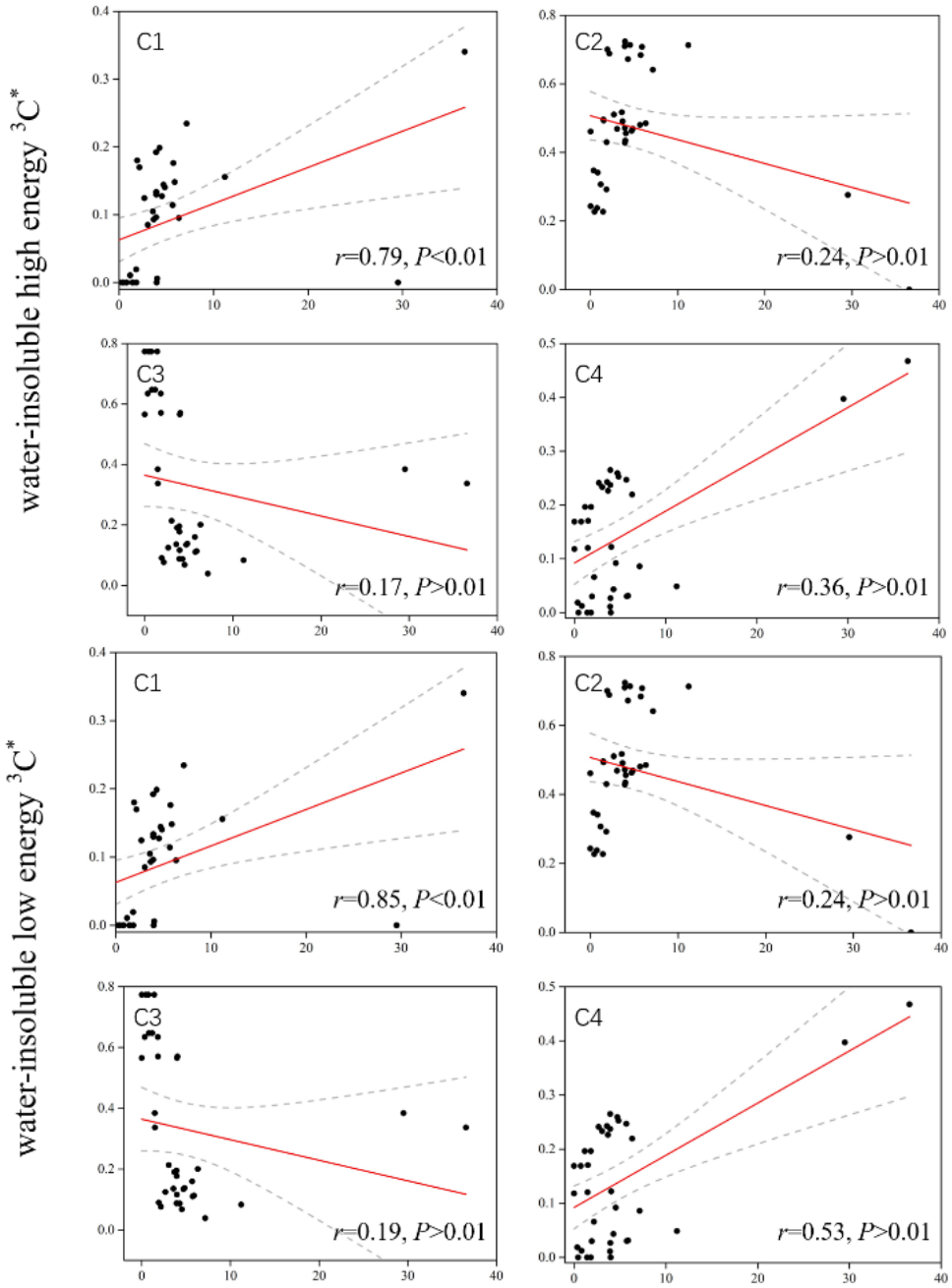

Fig.S19. (Continuous).

References

(1) Chen, Q. C., Fumikazu, I., Hayato, H., Daichi, A., Michihiro, M.: Chemical structural characteristics of HULIS and other fractionated organic matter in urban aerosols: results from mass spectral and FT-IR analysis, Environ. Sci. Technol., 50, 1721-1730, https://doi.org/10.1021/acs.est.5b05277, 2016.

(2) Utrya, N., Ajtaia, T., Filepa, Á., Pintera, M. D., Hofferb, A., Bozokia, Z., Szabo, G.: Mass specific optical absorption coefficient of HULIS aerosol measured by a four-wavelength photoacoustic spectrometer at NIR, VIS and UV wavelengths, Atmos. Environ., 69, 321-324, https://doi.org/10.1016/j.atmosenv.2013.01.003, 2013.

(3) Bodhipaksha, L. C., Sharpless, C. M., Chin, Y. P.: Triplet photochemistry of effluent and natural organic matter in whole water and isolates from effluentreceiving rivers, Environ. Sci. Technol., 49, 3453-3463, https://doi.org/10.1021/es505081w, 2015.

(4) Zhou, H. X., Yan, S. W., Ma, J. Z., Lian, L. S., Song, W. H.: Development of novel chemical probes for examining triplet natural organic matter under solar illumination, Environ. Sci. Technol., 51, http://dx.doi.org/10.1021/acs.est.7b02828, 11066-11074, 2017a.

(5) Maizel, A. C., Jing, L., Remucal, C. K.: Relationships between dissolved organic matter composition and photochemistry in Lakes of Diverse Trophic Status, Environ. Sci. Technol., 51, 9624-9632, http://dx.doi.org/10.1021/acs.est.7b01270, 2017.

(6) Laszakovits, J. R., Berg, S. M., Anderson, B. G.: p-Nitroanisole/Pyridine and p-Nitroacetophenone/Pyridine actinometers revisited: quantum yield in comparison to Ferrioxalate, Environ. Sci. Technol Lett., 4, 11-14, https://doi.org/10.1021/acs.estlett.6b00422, 2017.

(7) Mostafa, S., Rosario-Ortiz, F. L.: Singlet oxygen formation from wastewater organic matter, Environ. Sci. Technol., 47, 8179-8186., https://doi.org/10.1021/es401814s, 2013.

(8) Dalrymple, R. M., Carfagno, R. K., Sharpless, R. M.: Correlations between dissolved organic matter optical properties and quantum yields of singlet oxygen and hydrogen peroxide, Environ. Sci. Technol., 44, 5824-5829, https://doi.org/10.1021/es101005u, 2010.